Food & Function

Accepted Manuscript

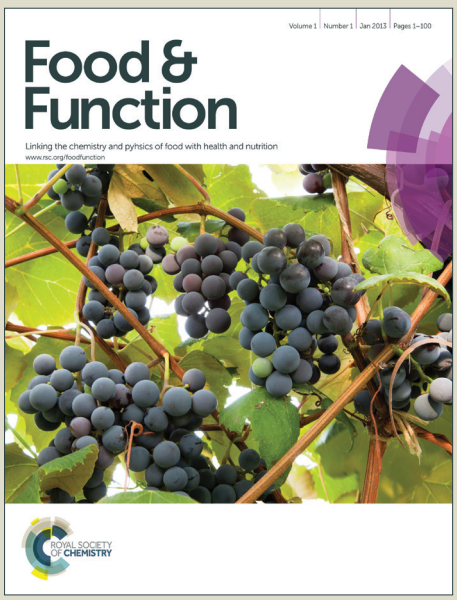

This is an *Accepted Manuscript*, which has been through the Royal Society of Chemistry peer review process and has been accepted for publication.

Accepted Manuscripts are published online shortly after acceptance, before technical editing, formatting and proof reading. Using this free service, authors can make their results available to the community, in citable form, before we publish the edited article. We will replace this *Accepted Manuscript* with the edited and formatted *Advance Article* as soon as it is available.

You can find more information about *Accepted Manuscripts* in the Information for Authors.

Please note that technical editing may introduce minor changes to the text and/or graphics, which may alter content. The journal's standard Terms & Conditions and the Ethical guidelines still apply. In no event shall the Royal Society of Chemistry be held responsible for any errors or omissions in this *Accepted Manuscript* or any consequences arising from the use of any information it contains.

ROYAL SOCIETY OF CHEMISTRY

www.rsc.org/foodfunction

Hypoglycemic effects of *Zanthoxylum* alkylamides by enhancing glucose metabolism and ameliorating pancreatic dysfunction in streptozotocin-induced diabetic rats

Yuming You, Ting Ren, Shiqi Zhang, Gerald Gasper Shirima, YaJiao Cheng and Xiong Liu*

College of Food Science, Southwest University, Chongqing, 400715, China

This study aimed to evaluate the hypoglycemic effect of *Zanthoxylum* alkylamides and explore the potential mechanism in streptozotocin (STZ)-induced diabetic rats. Diabetic rats were orally treated with 3, 6, and 9 mg kg^{-1} bw alkylamides daily for 28 days. As the alkylamides dose increased, the relative weights of the liver and kidney, fasting blood glucose, and fructosamine levels were significantly decreased. The alkylamides also significantly increased the body weight and improved the oral glucose tolerance of the rats. Likewise, the alkylamides significantly increased the levels of liver and muscle glycogen and plasma insulin. These substances further alleviated the histopathological changes in the pancreas of the diabetic rats. The beneficial effects of high-dose alkylamides showed a comparable activity to the anti-diabetic drug glibenclamide. Western blot and real-time PCR results revealed that the alkylamide treatment significantly decreased the expression levels of the key enzymes (phosphoenolpyruvate caboxykinase and glucose-6-phosphatase) involved in gluconeogenesis and increased glycolysis enzyme (glucokinase) in the liver, and enhanced the expression levels of pancreatic duodenal homeobox-1, glucokinase, and glucose transporter 2 in the pancreas. In addition, it was also observed that the alkylamides, unlike glibenclamide, increased the transient receptor potential cation channel subfamily V member 1 and decreased cannabinoid receptor 1 expressions in the liver and pancreas. Therefore, alkylamides can prevent STZ-induced hyperglycemia by altering the expression levels of the genes related to glucose metabolism and by ameliorating pancreatic dysfunction.

Introduction

Diabetes mellitus is a metabolic disorder characterized by chronic hyperglycemia that results from deficient insulin secretion and/or insulin resistance[1]. According to the statistics presented by the International Diabetes Federation in 2014, 8.3% of adults or 387 million individuals suffer from diabetes worldwide. Without intervention, the number of people with this disease will likely exceed 592 million by 2035[2]. Hence, the prevalence of diabetes is one of the most serious global health problems. Diabetes is treated using currently available agents, including insulin and various oral drugs, such as α-glucosidase inhibitors, metformin, and sulfonylureas. However, many of these agents produce adverse side effects after long-term use[3, 4]. Thus, safer and more effective components, especially from natural sources, should be developed.

Zanthoxylum schinifolium Sieb. et Zucc is an aromatic plant belonging to the genus *Zanthoxylum* of the family Rutaceae; this plant is mainly distributed in Sichuan, Chongqing, Hebei, Hunan, and Jilin in China, as well as in some Southeast Asian countries. The pericarps of *Z.schinifolium* is widely used as a seasoning spice in Asia because of the distinctive taste known as "ma," which is a tingling taste[5-7]. Unsaturated alkylamides, such as α-, β-,γ-, and δ-sanshool, and their analogues have been identified as the tingling taste-producing substances of *Zanthoxylum* species[8, 9]. The alkylamides from *Zanthoxylum* have shown extensive biological functions, including anticancer[10], anti-wrinkle[11], analgesic[12-14], digestive aid, and anti-inflammatory properties[15]. Previous studies demonstrated that alkylamides extracted from *Zanthoxylum* act as a transient receptor potential cation channel

subfamily V member 1 (TRPV1) activator and a cannabinoid receptor 1 (CB1) blocker[16-18]. TRPV1 and CB1 receptors play important roles in diabetes development; in particular, TRPV1 activator promotes insulin secretion and improves glucose homeostasis[19, 20]. The inhibition of CB1 receptor prevents apoptosis of β-cells under stress caused by obesity and streptozotocin (STZ) toxicity[21]. The two receptors also regulate energy expenditure in peripheral organs[22]. Therefore, alkylamides exhibit promising hypoglycemic properties. However, studies have yet to investigate the hypoglycemic properties and possible mechanism of *Zanthoxylum* alkylamides.

In this study, alkylamides were extracted from a highly tingling active supercritical fluid (SCF) extract prepared from the dried pericarps of *Z. Schinifolium*, to evaluate the hypoglycemic effects and potential mechanism in STZ-induced diabetic rats.

Materials and methods

Alkylamide extraction and identification

Alkylamides were extracted from the SCF extract (Jiangjin Four Mountain Company, Chongqing, China) isolated from the dried pericarps of *Z. Schinifolium* through supercritical carbon dioxide extraction. The SCF extract (20 g) was mixed with 40 g of a heated water-free silica gel chromatograph and then soaked in 200 mL of anhydrous ether at room temperature for 2 h to remove essential and non-essential oils. After anhydrous ether was volatilized, the mixture was extracted with 200 mL of methanol at 55 °C for 6 h and then filtered. The filtrate was evaporated *in vacuo* to yield a crude extract. The crude extract was refluxed with 50 mL of petroleum ether overnight. The supernatant was collected and crystallized at −20 °C. The resultant

suspension was dried using a drying N_2 gas at low temperature; as a result, white powder was produced.

The individual alkylamides were identified through HPLC-UV/MS in accordance with a previous report with slight modifications[23]. The alkylamides (10 mg/mL in methanol) were analyzed using a Shidmadzu LC-20A system (Shidmadzu Corp., Tokyo, Japan) equipped with a diode array detector (DAD) and an API 4000 QTRAP mass spectrometer system (AB Sciex, Darmstadt, Germany). The samples were applied to a C_{18} column (4.6 mm × 250 mm, 5 μm, Phenomenex Ltd., Guangzhou, China) and eluted with a gradient mobile phase composed of water (phase A) and acetonitrile (phase B) at a flow rate of 500 μL/min. The linear gradient program of phase B started from 35%, increased to 75% from 0 min to 30 min, and further increased to 100% when the time was 40 min; the program was maintained at 100% from 40 min to 45 min and then decreased from 100% to 35% from 45 min to 50 min. The wavelength range of the DAD was set as 200 nm to 700 nm. The API 4000 QTRAP LC-MS was fitted with an electrospray ionization source and a triple quadrupole-ion trap mass analyzer. The following parameters were set: nitrogen pressure, 30 psi; turbo ion spray probe, 400°C; ion spray voltage, 4500 V, positive mode; declustering potential, 450 V; entrance potential, 6 V; and collision energy, 10 V. Ions were scanned from *m*/*z* 100 to *m*/*z* 1000.

Experimental animals

6-8 weeks old male Sprague–Dawley rats were obtained from Chongqing Tengxin Laboratory Animal, Inc. (Chongqing, China). The rats were housed in stainless steel

screen bottom cages (two rats per cage) at an ambient temperature of 25 ± 2 °C with 12 h/12 h light/dark cycle. The rats were allowed free access to standard diet (Chongqing Tengxin Laboratory Animal, Inc., Chongqing, China) and water *ad libitum*. The rats were acclimatized to the laboratory environment for one week. Experiments were performed in accordance with the institutional regulations and national criteria for the use of laboratory animals and approved by the Animal Care and Use Committee of Southwest University.

Diabetes induction and experimental design

After the rats were subjected to an overnight fasting, the rats were intraperitoneally injected with 60 mg kg^{-1} bw STZ (Sigma Chemicals, St. Louis, MO, USA) dissolved in 0.1 mol/L of citrate buffer (pH 4.5)[24]. The rats in the normal control group were treated with the same volume of citrate buffer. Three days after STZ was injected, the fasting blood glucose (FBG) of the rats was measured from the tail tip. The rats with FBG levels above 11.1 mmol/L were used as diabetic rats for further study.

The experiments involving the rats were carried out after STZ was injected for one week. Forty-eight rats were randomly divided into six groups with eight rats in each group. The positive group (600 μg kg^{-1} bw): diabetic rats treated with 0.2 mL per 100 g bw of soybean oil containing 300 μg/mL glibenclamide. Diab-LD (3 mg kg^{-1} bw), diab-MD (6 mg kg^{-1} bw) and diab-HD (9 mg kg^{-1} bw) group: diabetic rats treated with 0.2 mL per 100 g bw of soybean oil containing 1.5, 3, and 4.5 mg/mL alkylamides, respectively. The normal and diabetic model groups received equivalent amounts of soybean oil. The rats were orally treated once daily via an intragastric tube

for 28 days.

Experimental and sampling procedures

Body weight was measured every two days. FBG was examined on days 0, 14, and 28 of the experiment. Oral glucose tolerance test (OGTT) was performed on day 27 of the treatment. The rats were fasted for 12 h and treated with 2 g kg^{-1} bw of glucose via orogastric gavage. Blood was collected from the tail vein at 0, 30, 60, 90, and 120 min after glucose was administered. On the last day of the experimental period, the rats were sacrificed through decapitation after these rats were subjected to an overnight fasting. Blood was collected from the neck and then placed in a blood collection tube (Shandong Aosite Medical Instrument Factory, Shandong, China) containing heparin sodium as an anticoagulant. The plasma was separated through centrifugation at 1400 × *g* at 4°C for 15 min and then stored at −80 °C until analysis. The liver, kidney, pancreas, and muscle tissues of each rat were immediately excised, washed with ice-cold saline, dried, weighed, transferred to liquid nitrogen, and stored at −80 °C for further analysis.

Biochemical assay

FBG and fructosamine (FMN) levels in the plasma were determined using a commercially available kit (Sichuan Maker Biotechnology Co., Ltd., Sichuan, China) on a Hitachi 7020 automatic biochemistry analyzer (Hitachi High-Technologies Corp., Tokyo, Japan). The plasma insulin and glycogen content of the liver and muscle tissues were determined using an enzyme linked immunoabsorbent assay kit and a glycogen kit, respectively (Nanjing Jiancheng Bioengineering Institute, Nanjing,

China), in accordance with the manufacturer's protocols.

RNA extraction and quantitative RT-PCR analysis

Frozen tissues were homogenized in 1 mL of RNAiso Plus (TaKaRa Bio, Otsu, Japan) by using TissueLyser II (Qiagen, Hilden, Germany) at 30 Hz for 4 min. Total RNA was extracted in accordance with the manufacturer's recommendations. RNA concentration and purity were quantified using a NanoDrop 1000 spectrophotometer (Thermo Scientific, Delaware, USA). The integrity of RNA was verified through agarose gel electrophoresis by using a Gel Doc XR^+ system (Bio-Rad, Hercules, CA, USA). Afterward, 2 μg of RNA was reverse transcribed to cDNA by using a PrimeScript RT reagent kit (TaKaRa Bio, Otsu, Japan). The genes of TRPV1, CB1, glucokinase (GK), glucose-6-phosphatase (G6Pase), phosphoenolpyruvate caboxykinase (PEPCK), pancreatic duodenal homeobox-1 (PDX-1), and glucose transporter 2 (GLUT2) were analyzed through RT-PCR by using the Light Cycler Nano Instrument (Life Technologies, USA). The reaction mixture (20 μL) contained 10 μL of SYBR Premix Ex *Taq*II (TaKaRa Bio, Otsu, Japan), 1 μL of forward primer (10 μmol/L), 1 μL of reverse primer (10 μmol/L), and 2 μL of cDNA. The real-time PCR protocol was conducted as follows: 95 °C for 10 min and 45 cycles of 95 °C for 10 s, 55 °C for 20 s, and 72 °C for 30 s. The sequences of the primers (Sangon Biological Engineering, Shanghai, China) used in the experiments are shown in Table 1. Gene expression data were normalized to β-actin, and the relative expression level of each gene was calculated using the $2^{-\Delta\Delta Ct}$ method.

Western blot analysis of the target proteins

The liver and pancreas samples collected from each group were homogenized in an ice-cold lysed buffer. The suspensions were centrifuged at 14,000 × *g* at 4 °C for 15 min. The protein content was determined using the BCA method. The proteins were separated by 12% SDS-PAGE and then transferred to a 0.45 μm PVDF membrane (Millipore Corp., USA). The membranes were blocked with 5% defatted milk powder for 1 h and incubated with anti-PEPCK, anti-G6Pase, anti-GK, anti-PDX, anti-GLUT2, anti-TRPV1, or anti-CB1 (Abcam Inc., USA) antibodies for 1 h at 37 °C. Afterward, the membranes were washed with TBST and incubated with horseradish peroxidase-conjugated secondary antibodies (Santa Cruz, USA) at 37 °C for 1 h. After the membrane was washed with TBST, the proteins were visualized through ECL (Millipore Corp., USA); the expression level was determined using Quantity One software (Bio-Rad, USA).

Histopathological examination

A part of the pancreatic tissues were fixed in a Bouin solution for 24 h and then stored in 70% ethanol until histological analysis. A portion of the stored tissue was embedded in paraffin, cut into 5 μm thick sections by using a microtome (Leica, Wetzlar, Germany), stained with hematoxylin and eosin (HE), and observed under an Olympus BX43 light microscope (Olympus Corp., Tokyo, Japan) coupled with a high-resolution digital camera.

Statistical analysis

Results were expressed as mean ± standard error and analyzed by one-way analysis of variance (ANOVA). Student's *t* test was used to detect the differences in the means

between the normal group and the diabetic rat group. Differences were considered significant when $P<0.05$. Data were processed using SPSS 21.0 and Origin 8.1.

Results

HPLC-UV/MS analysis of alkylamides

HPLC-UV/MS was performed to identify the individual alkylamides present in the extracts. The peaks were identified by comparing the UV absorption and MS spectra with the published data. On the basis of the HPLC chromatogram and mass spectra of the extracts shown in Fig.1, we found that the three main peaks exhibited a maximal UV absorption at approximately 270 nm, which is consistent with the presence of an aliphatic-conjugated double bond system and fits well with the data reported for sanshool derivatives[13]. Peaks 1 and 2 yielded UV λ_{max} of 262, 272, and 283 and revealed an $[M+H]^+$ ion at *m/z* 264; this result indicated that the two compounds were isomers, which correspond to hydroxy-α-sanshool and hydroxy-β-sanshool, respectively[13, 23]. Peak 3 was identified as hydroxy-γ-sanshool with UV λ_{max} of 265, 275, and 283, and $[M+H]^+$ ion at *m/z* 290[25, 26].

Effect of alkylamides on body weight and relative weight of organs

The changes in the body weight of the experimental rats are shown in Table 2. After four weeks, the diabetic model rats showed less body weight gain (6.37%) than the normal rats (29.21%). The body weight gain was significantly increased when the rats were treated with alkylamides and glibenclamide. Table 2 also shows the relative weight of the organs of the experimental rats after four weeks. After the rats were treated with alkylamides, the relative weight of the pancreas decreased, but the

difference was not significant. Compared with the normal rats, the STZ-induced diabetic rats showed a significant increase in the relative weights of the liver and the kidney. By contrast, the weights of the liver and the kidney were considerably decreased when alkylamides and glibenclamide were administered.

Effect of alkylamides on FBG and fructosamine

The initial FBG level of the STZ-induced diabetic rats was markedly increased compared with that of the normal group, and there were no significant differences in the glucose level among the diabetic rats (Fig. 2A). However, the FBG level of the rats in alkylamide- and glibenclamide-treated groups were significantly decreased after two weeks of the experiment. Compared with the FBG level of the diabetic model rats, the FBG level of the rats in diab-LD, diab-MD, and diab-HD groups were respectively reduced by 8.83%, 20.77%, and 23.83% after 14 days; the FBG level of the rats in diab-LD, diab-MD, and diab-HD groups were further reduced respectively by 18.14%, 32.33%, and 36.68% after 28 days.

Fructosamine is related to the average content of glucose during the first three weeks; this parameter was considered as an earlier indicator of the diagnosis of ambient glycemia compared with HbA_{1c}[27]. Therefore, plasma fructosamine concentrations were measured in the experimental rats. The fructosamine level was significantly higher in diabetic model rats than in the normal control group at the end of the study. The alkylamide treatment significantly decreased the fructosamine level of the diabetic rats by 5.20%, 10.4%, and 12.72% when low-, medium-, and high-dose alkylamides were respectively administered. Glibenclamide also significantly

decreased the fructosamine level in diabetic rats, but glibenclamide did not significantly differ from the high-dose alkylamide administered to the rats (Fig. 2B).

Effect of alkylamides on OGTT

OGTT was performed using the experimental rats after these rats were subjected to fasting for 12 h on day 27. In normal rats, the blood glucose level returned to the initial level at 120 min after glucose was administered (Fig. 3A). In the diabetic model rats, the blood glucose levels remained higher than the initial level even after 120 min. Low-, medium-, and high-dose alkylamides induced a significant decrease at 60, 90, and 120 min after glucose was administered. Diab-MD-, diab-HD-, and the glibenclamide-treated rats did not significantly differ from one another. The AUC indicated a significant restoration of the glucose tolerance and homeostasis when the rats were treated with alkylamides and glibenclamide compared with the diabetic model rats (Fig. 3B).

Effect of alkylamides on plasma insulin and tissue glycogen

The plasma insulin level was significantly decreased in the diabetic model rats compared with the normal rats (Fig. 4A). After 28 days of alkylamide and glibenclamide treatment, alkylamides significantly increased the diabetic-induced decrease in the plasma insulin levels; among the three doses, the high-dose alkylamide treatment was the most beneficial; the beneficial effect of the high-dose alkylamide treatment was also significantly greater than that of glibenclamide. After the rats were treated with high-dose alkylamide, the plasma insulin level was almost similar to that of the normal group (24.70 ± 1.30 μIU/mL and 26.93 ± 1.08 μIU/mL).

Similar results were observed in the glycogen content of the liver and muscle tissues (Fig. 4B). Medium- and high-dose alkylamides significantly increased the glycogen contents to an extent similar to that of glibenclamide.

Histopathological changes in the pancreas

Histopathological changes in the pancreas of the experimental rats were observed through HE staining after 28 days of treatment (Fig. 5). A complete pancreatic islet structure exhibiting regular distribution, β-cell-granulated cytoplasm, and uniform nuclei was detected in the normal rats. By contrast, the pancreatic islets of the diabetic model rats were atrophic and damaged, and the number and size of β-cells were reduced. Alkylamide and glibenclamide treatments markedly ameliorated these histopathological changes and elicited a distinct granulated and protective effect on β-cells.

Effect of alkylamide on the mRNA and protein levels of key genes in liver and pancreas

The mRNA and protein expression levels of the genes related to glucose metabolism and insulin signaling and other relevant genes in the liver and pancreas tissues were investigated to understand the mechanism by which alkylamides elicit a hypoglycemic effect on STZ-induced diabetic rats (Fig. 6 and 7). The mRNA and protein expression levels of pancreatic PDX-1, GLUT2, and GK and hepatic GK were significantly decreased; by contrast, the mRNA and protein expression levels of hepatic PEPCK and G6Pase were remarkably upregulated in the diabetic model rats (Fig. 6A, B and C, 7A, B and C). After the rats were treated with alkylamides and

glibenclamide, the expression levels of pancreatic PDX-1, GK, and GLUT2 were significantly higher than those of the diabetic model rats (Fig. 7A, B and C). Compared with the diabetic model rats, the rats treated with alkylamides and glibenclamide also exhibited a remarkable increase in the hepatic GK level and a significant decrease in the expression levels of hepatic PEPCK and G6Pase (Fig. 6A , B and C).

The expression levels of CB1 in hepatic and pancreatic tissues were significantly increased in the diabetic rats. After the rats were treated with alkylamides, the expression levels of TRPV1 in hepatic and pancreatic tissues were significantly upregulated; by contrast, the expression levels of CB1 were remarkably downregulated. These changes in TRPV1 and CB1 levels were not found in the glibenclamide-treated group (Fig. 6D, E and F, 7D, E and F).

Discussion

Diabetes mellitus is often associated with hyperglycemia, defects in insulin secretion, and reduced pancreatic β-cell mass[28]. STZ is widely used to induce experimental type I diabetes, and this substance can damage pancreatic β cells and cause a decreased insulin release[29, 30]. These events then lead to hyperglycemia. In this study, the STZ-induced diabetic rats exhibited a notable increase in FBG and relative weight of organs (Table 2); this finding is consistent with that observed in previous studies[31, 32]. However, the alkylamide treatment for 28 days reversed organs enlargement, caused an evident decrease in the levels of FBG, plasma fructosamine, and improved oral glucose intolerance; these changes in the parameters indicated the hypoglycemic

296 effect of alkylamides. Similar to alkylamides, glibenclamide elicited a significant
297 hypoglycemic effect on the STZ-induced diabetic rats. As an orally anti-diabetic drug,
298 glibenclamide is often used as a positive drug in STZ-induced diabetic models to
299 compare the anti-diabetic properties of various natural compounds. Serrano-Martin *et*
300 *al.*[33] indicated that glibenclamide increases insulin secretion by blocking the
301 ATP-sensitive potassium channels in pancreatic β-cells; as a result, membrane
302 depolarization and stimulation of Ca^{2+} influx, an initial key step in insulin release,
303 however, the risk of hypoglycemia increases, particularly in elderly people[34]. In our
304 study, side effects were not observed in the alkylamide-treated rats; therefore,
305 alkylamides can be safely administered.

306 Increased endogenous glucose production is a common abnormality associated with
307 diabetes. The liver is the main site that maintains the balance between glucose use and
308 storage by regulating glycolysis and gluconeogenesis[35, 36]. In our study, the levels of
309 blood glucose and hepatic glycogen were significantly reversed after the rats were
310 treated with alkylamides (Fig. 2A and 4B). On the basis of these findings, we
311 hypothesized that alkylamides may modulate the critical enzymes of glycolysis and
312 glycogen synthesis in the liver. GK, which catalyzes the phosphorylation of glucose to
313 glucose-6-phosphate, is the first rate-limiting enzyme in glucose oxidation. PEPCK is
314 a crucial enzyme of gluconeogenesis; this enzyme catalyzes the synthesis of
315 glucose-6-phosphate from non-carbohydrate precursors. G6Pase catalyzes the
316 dephosphorylation of glucose-6-phosphate to glucose, and this reaction is the last step
317 in gluconeogenesis and glycogenolysis. Previous studies indicated that GK, PEPCK,

and G6Pase are the most sensitive indicators of endogenous glucose production in the diabetic state[37-39]. The reduced GK level and the enhanced expression levels of PEPCK and G6Pase in the liver are likely responsible for the increase in endogenous glucose associated with diabetes[40]. Our results indicated that alkylamide treatment increased the GK expression and downregulated PEPCK and G6Pase expression levels in the liver of diabetic rats (Fig. 6A and B). These findings suggested that the mediated hepatic glucose metabolism and gluconeogenesis via the reversal of the expression levels of GK, PEPCK, and G6Pase genes may be the functional mechanism operated by alkylamides in the STZ-induced diabetic rats.

Insulin deficiency plays an important role in the development of type I diabetes. The hypoglycemic property of some bioactive components are mainly induced by protecting the pancreatic islets and by improving insulin secretion[41-43]. Pancreas development, β-cell differentiation, and mature β-cell functioning are significantly mediated by PDX-1[44]. During pancreas development, PDX-1 is expressed in precursor cells and then becomes restricted to β-cells. In mature β-cells, PDX-1 is considered as a key transcription factor of insulin gene and other genes, such as GLUT2 and GK, related to glucose sensing and metabolism[45, 46]. In the present study, followed with the damage of the pancreatic β-cells by STZ, the expression levels of PDX-1, GLUT2, and GK were remarkably downregulated in the pancreas. As a result, the decreased plasma insulin level and hyperglycemia. After the diabetic rats were treated with high-dose alkylamides, the decreased PDX-1, GLUT2, and GK expression levels and plasma insulin level were almost restored to the normal level

(Fig. 4A, 7A, B and C); this result indicated that alkylamides can protect pancreatic β-cells from STZ-induced damage. This hypothesis was further confirmed by the results of the histopathological examination of the pancreas (Fig. 5).

The roles of TRPV1 and CB1 receptors in diabetes, obesity, metabolic syndrome, and cardiovascular diseases have been described[47-49]. TRPV1 interacts with CB1; in this interaction, receptors undergo "cross-talking."[50] Glucose-mediated insulin release is increased in INS-1E cells when CB1 receptors are blocked with an inverse agonist and TRPV1 receptors are maintained in a sensitized responsive state[51]. These findings indicated that the regulation of TRPV1 and CB1 receptors may be a novel method to treat diabetes. Our study is the first to demonstrate that alkylamide treatment significantly downregulated CB1 expression level and upregulated TRPV1 expression level in diabetic rats (Fig. 6D, E and F, 7D, E and F). Hence, alkylamides in the liver and pancreas may mediate CB1 and TRPV1 expression levels and affect the enzymatic expression of glucose metabolism-related genes, such as PEPCK, GK, and PDX-1. However, further studies should be conducted to verify this hypothesis.

Conclusion

The hypoglycemic effect of the alkylamides extracted from *Zanthoxylum* may be attributed to the modulation of hepatic glucose metabolism and gluconeogenesis by upregulating or downregulating the expression levels of key enzymes, such as PEPCK, GK, and G6Pase in STZ-induced diabetic rats. Alkylamide treatment could also repair the damaged pancreatic β-cells and upregulate the expression levels of PDX-1, GK, and GLUT2 in the pancreas; as a result, plasma insulin level may be almost restored

362 to normal levels. Although alkylamides may provide many health benefits for diabetic
363 individuals, the alkylamides used in the study are a mixture of hydroxy-α-sanshool,
364 hydroxy-β-sanshool, and hydroxy-γ-sanshool. Further studies should be conducted to
365 isolate individual components and characterize the corresponding beneficial
366 biological properties.
367
368 **Abbreviations**

369	CB1	Cannabinoid receptor 1
370	DAD	Diode array detector
371	FBG	Fasting blood glucose
372	FMN	Fructosamine
373	G6pase	Glucose-6-phosphatase
374	GK	Glucokinase
375	GLUT2	Glucose transporter 2
376	OGTT	Oral glucose tolerance test
377	PDX-1	Pancreatic duodenal homeobox-1 and
378	PEPCK	Phosphoenolpyruvate caboxykinase,
379	SCF	Supercritical fluid
380	STZ	Streptozotocin
381	TRPV1	Transient receptor potential cation channel subfamily V member 1

382
383 **Acknowledgments** This work was supported by the National Natural Science

Foundation of China (NSFC 31171679).

References

1. B. Sarmadi, F. Aminuddin, M. Hamid, N. Saari, A. Abdul-Hamid and A. Ismail, *Food Chem*, 2012, **134**, 905-911.
2. IDF, *http://www.idf.org/diabetesatlas*, 2014.
3. J. Zhu, W. Liu, J. P. Yu, S. Zou, J. J. Wang, W. B. Yao and X. D. Gao, *Carbohyd Polym*, 2013, **98**, 8-16.
4. S. E. Inzucchi, *Jama-J Am Med Assoc*, 2002, **287**, 360-372.
5. X. G. Yang, *J Agr Food Chem*, 2008, **56**, 1689-1696.
6. W. R. Diao, Q. P. Hu, S. S. Feng, W. Q. Li and J. G. Xu, *J Agr Food Chem*, 2013, **61**, 6044-6049.
7. Y. J. Zhang, D. M. Wang, L. N. Yang, D. Zhou and J. F. Zhang, *Plos One*, 2014, **9**.
8. E. Sugai, Y. Morimitsu and K. Kubota, *Biosci Biotech Bioch*, 2005, **69**, 1958-1962.
9. C. Menozzi-Smarrito, C. E. Riera, C. Munari, J. Le Coutre and F. Robert, *J Agr Food Chem*, 2009, **57**, 1982-1989.
10. K. P. Devkota, J. Wilson, C. J. Henrich, J. B. McMahon, K. M. Reilly and J. A. Beutler, *Journal of natural products*, 2013, **76**, 59-63.
11. C. Artaria, G. Maramaldi, A. Bonfigli, L. Rigano and G. Appendino, *Int J Cosmetic Sci*, 2011, **33**, 328-333.
12. M. Tsunozaki, R. C. Lennertz, D. Vilceanu, S. Katta, C. L. Stucky and D. M. Bautista, *J Physiol-London*, 2013, **591**, 3325-3340.
13. K. Mizutani, Y. Fukunaga, O. Tanaka, N. Takasugi, Y. Saruwatari, T. Fuwa, T. Yamauchi, J. Wang, M. R. Jia, F. Y. Li and Y. K. Ling, *Chem Pharm Bull*, 1988, **36**, 2362-2365.
14. V. Iseli, O. Potterat, L. Hagmann, J. Egli and M. Hamburger, *Pharmazie*, 2007, **62**, 396-400.
15. K. C. Albin and C. T. Simons, *Plos One*, 2010, **5**.
16. E. Sugai, Y. Morimitsu, Y. Iwasaki, A. Morita, T. Watanabe and K. Kubota, *Biosci Biotech Bioch*, 2005, **69**, 1951-1957.
17. C. E. Riera, C. Menozzi-Smarrito, M. Affolter, S. Michlig, C. Munari, F. Robert, H. Vogel, S. A. Simon and J. le Coutre, *Brit J Pharmacol*, 2009, **157**, 1398-1409.
18. K. S. S. Dossou, K. P. Devkota, C. Morton, J. M. Egan, G. H. Lu, J. A. Beutler and R. Moaddel, *Journal of natural products*, 2013, **76**, 2060-2064.
19. D. X. Gram, B. Ahren, I. Nagy, U. B. Olsen, C. L. Brand, F. Sundler, R. Tabanera, O. Svendsen, R. D. Carr, P. Santha, N. Wierup and A. J. Hansen, *Eur J Neurosci*, 2007, **25**, 213-223.
20. P. J. Wang, Z. C. Yan, J. Zhong, J. Chen, Y. X. Ni, L. Li, L. Q. Ma, Z. G. Zhao, D. Y. Liu and Z. M. Zhu, *Diabetes*, 2012, **61**, 2155-2165.
21. W. Kim, Q. Z. Lao, Y. K. Shin, O. D. Carlson, E. K. Lee, M. Gorospe, R. N. Kulkarni and J. M. Egan, *Sci Signal*, 2012, **5**.
22. C. Li, P. M. Jones and S. J. Persaud, *Pharmacol Therapeut*, 2011, **129**, 307-320.
23. Z. F. Zhao, R. X. Zhu, K. Zhong, Q. He, A. M. Luo and H. Gao, *J Food Sci*, 2013, **78**, C1516-C1522.
24. M. P. Riya, K. A. Antu, S. Pal, A. K. Srivastava, S. Sharma and K. G. Raghu, *Food Funct*, 2014, **5**,

2086-2095.
25. Q. B. Xiong, D. W. Shi, H. Yamamoto and M. Mizuno, *Phytochemistry*, 1997, **46**, 1123-1126.
26. M. Bader, T. D. Stark, C. Dawid, S. Losch and T. Hofmann, *J Agr Food Chem*, 2014, **62**, 2479-2488.
27. H. Malmstrom, G. Walldius, V. Grill, I. Jungner, S. Gudbjornsdottir and N. Hammar, *Plos One*, 2014, **9**.
28. N. Ktari, K. Mnafgui, R. Nasri, K. Hamden, I. Bkhairia, A. Ben Hadj, T. Boudaouara, A. Elfeki and M. Nasri, *Food Funct*, 2013, **4**, 1691-1699.
29. B. Sharma, C. Balomajumder and P. Roy, *Food Chem Toxicol*, 2008, **46**, 2376-2383.
30. H. J. Kim, I. G. Chae, S. G. Lee, H. J. Jeong, E. J. Lee and I. S. Lee, *J Ginseng Res*, 2010, **34**, 104-112.
31. C. Tourrel, D. Bailbe, M. J. Meile, M. Kergoat and B. Portha, *Diabetes*, 2001, **50**, 1562-1570.
32. M. Zafar and S. N. U. H. Naqvi, *Int J Morphol*, 2010, **28**, 135-142.
33. X. Serrano-Martin, G. Payares and A. Mendoza-Leon, *Antimicrob Agents Ch*, 2006, **50**, 4214-4216.
34. G. Derosa and P. Maffioli, *International Journal of Diabetes in Developing Countries*, 2014, **34**, 61-68.
35. C. H. Lin, Y. H. Kuo and C. C. Shih, *Int J Mol Sci*, 2014, **15**, 20022-20044.
36. M. X. Xie, D. L. Chen, F. Zhang, G. R. Willsky, D. C. Crans and W. J. Ding, *J Inorg Biochem*, 2014, **136**, 47-56.
37. D. Argaud, Q. Zhang, W. S. Pan, S. Maitra, S. J. Pilkis and A. J. Lange, *Diabetes*, 1996, **45**, 1563-1571.
38. H. Y. Hung, K. D. Qian, S. L. Morris-Natschke, C. S. Hsu and K. H. Lee, *Nat Prod Rep*, 2012, **29**, 580-606.
39. P. L. Huang, C. W. Chi and T. Y. Liu, *Food Chem Toxicol*, 2013, **55**, 137-143.
40. A. L. de la Garza, U. Etxeberria, S. Palacios-Ortega, A. G. Haslberger, E. Aumueller, F. I. Milagro and J. A. Martinez, *Food Funct*, 2014, **5**, 2120-2128.
41. Z. J. Zhang, J. Jiang, P. Yu, X. P. Zeng, J. W. Larrick and Y. Q. Wang, *J Transl Med*, 2009, **7**.
42. Y. L. Wang, Z. Q. Xiao, S. Liu, L. S. Wan, Y. D. Yue, Y. T. Zhang, Z. X. Liu and J. C. Chen, *J Ethnopharmacol*, 2013, **150**, 536-544.
43. K. Rashid and P. C. Sil, *Toxicol Appl Pharm*, 2015, **282**, 297-310.
44. H. Kaneto, T. Miyatsuka, Y. Fujitani, H. Noguchi, K. H. Song, K. H. Yoon and T. A. Matsuoka, *Diabetes Res Clin Pr*, 2007, **77**, S127-S137.
45. M. Lotfy, J. Singh, H. Rashed, S. Tariq, E. Zilahi and E. Adeghate, *J Endocrinol*, 2014, **220**, 291-304.
46. Y. Zhang, C. J. Ren, G. B. Lu, Z. M. Mu, W. Z. Cui, H. J. Gao and Y. W. Wang, *Int Immunopharmacol*, 2014, **22**, 248-257.
47. Y. B. Zhu, J. Gao and D. W. Zou, *J Gastroen Hepatol*, 2013, **28**, 745-745.
48. A. Mohammadi-Farani, M. Ghazi-Khansari and M. Sahebgharani, *Iran J Basic Med Sci*, 2014, **17**, 673-678.
49. P. Pacher, S. Batkai and G. Kunos, *J Physiol-London*, 2004, **558**, 647-657.
50. R. M. Evans, R. H. Scott and R. A. Ross, *Brit J Pharmacol*, 2007, **152**, 404-413.
51. K. Malenczyk, M. Jazurek, E. Keimpema, C. Silvestri, J. Janikiewicz, K. Mackie, V. Di Marzo, M. J. Redowicz, T. Harkany and A. Dobrzyn, *J Biol Chem*, 2013, **288**, 32685-32699.

469 **Tables**

470 **Table 1 primer sequence and product size**

Gene	Primer sequence		Product size
	Forward primer	Reverse primer	
β-actin	ACGTCAGGTCATCACTATCG	GGCATAGAGGTCTTTACGGATG	154
TRPV1	GGTTCACTCCTGACGGCAAG	GCCTGGGTCCTCGTTGATG	107
CB1	CTGAGGAGCAAGGACCTGAGAC	GTTGTTGGCGTGCTTGTGC	120
GK	GCTTTTGAGACCCGTTTCGT	CGCACAATGTCGCAGTCG	119
G6Pase	GGCTCACTTTCCCCATCAGGT	CCAAGTGCGAAACCAAACAGG	144
PEPCK	GACAGACTCGCCCTATGTGGTG	GGTTGCAGGCCCAGTTGTTG	161
PDX-1	AAACGCCACACACCAAGGAGAA	AGACCTGGCGGTTCACATG	152
GLUT2	CCAGCACATACGACACCAGACG	CCAAAGAACGAGGCGACCAT	125

471

472

473 **Table 2 Body weight and weight of organs in diabetic rats treated with alkylamides[a]**

	Body weight (g)			Relative weight of organs		
	Initial	Final	Gain	Liver (%)	Kidney (%)	Pancreas (%)
Control	259.29±10.82	334.86±16.49	75.75±7.08	2.76±0.14	0.67±0.02	0.20±0.03
Diabetic	206.43±6.42	219.57±11.06	13.14±5.70$^{\#a}$	4.03±0.14$^{\#a}$	0.95±0.04$^{\#a}$	0.22±0.04
Diab-LD	203.29±7.08	223.86±7.74	20.57±1.77^{ab}	3.65±0.25^{b}	0.85±0.03^{b}	0.21±0.07
Diab-MD	221.13±4.27	258.63±5.24	37.50±4.55^{b}	3.30±0.14^{c}	0.80±0.02^{b}	0.20±0.06
Diab-HD	208.25±4.93	247.50±10.67	39.25±7.16^{b}	3.28±0.17^{c}	0.79±0.02^{b}	0.20±0.03
Diab-Gliben	219.86±5.10	254.71±3.58	34.86±2.37^{b}	3.09±0.11^{c}	0.81±0.02^{b}	0.21±0.05

474 [a]Values are the mean ± S.E.M (n = 8). Control: normal rats treated with vehicle; Diabetic: diabetic
475 rats treated with vehicle; Diab-LD, diabetic rats treated with 3 mg kg^{-1} bw alkylamides; Diab-MD:
476 diabetic rats treated with 6 mg kg^{-1} bw alkylamide; Diab-HD, diabetic rats treated with 9 mg kg^{-1}
477 bw alkylamide; Diab-Gliben: diabetic rats treated with 600 μg kg^{-1} bw glibenclamide. Means with
478 different superscript letters are significantly different among the diabetic rats (P< 0.05); $^{\#}$ means
479 are significantly different (P<0.05) than the means in the control group.

480

Figure captions

Fig. 1 HPLC-DAD chromatogram of alkylamides extracted from *Zanthoxylum* (a) and mass spectra for peak 1 (b), peak 2 (c) and peak 3 (d), respectively.

Fig.2 Fasting blood glucose (FBG) (A) and fructosamine level (B) in diabetic rats treated with alkylamides. Data are expressed as mean ± S.E.M (n = 8). Control: normal rats treated with vehicle; Diabetic: diabetic rats treated with vehicle; Diab-LD, diabetic rats treated with 3 mg kg^{-1} bw alkylamides; Diab-MD: diabetic rats treated with 6 mg kg^{-1} bw alkylamide; Diab-HD, diabetic rats treated with 9 mg kg^{-1} bw alkylamide; Diab-Gliben: diabetic rats treated with 600 μg kg^{-1} bw glibenclamide. Means with different superscript letters are significantly different among the diabetic rats (P< 0.05); $^{\#}$ means are significantly different (P<0.05) than the means in the control group.

Fig.3 Oral glucose tolerance test (OGTT) (A) and area of under curve (AUC) (B) in diabetic rats treated with alkylamides. Data are expressed as mean ± S.E.M (n = 8). Conditions were as defined in Figure 2. Means with different superscript letters are significantly different among the diabetic rats (P< 0.05); $^{\#}$ means are significantly different (P<0.05) than the means in the control group.

Fig. 4 Plasma insulin (A) and glycogen level (B) in diabetic rats treated with alkylamides. Data are expressed as mean ± S.E.M (n = 8). Conditions were as defined in Figure 2. Means with different superscript letters are significantly different among the diabetic rats (P< 0.05); $^{\#}$ means are significantly different (P<0.05) than the means in the control group.

Fig.5 Changes in histopathology of pancreas in diabetic rats treated with alkylamides (HE staining, scale bar: 200 μm). (A) normal control rats, (B) diabetic model rats, (C) diabetic rats treated with 3 mg kg^{-1} bw alkylamides, (D) diabetic rats treated with 6 mg kg^{-1} bw alkylamides, (E) diabetic rats treated with 9 mg kg^{-1} bw alkylamides, (F) diabetic rats treated with 600 μg kg^{-1} bw glibenclamide.

Fig. 6 Glucose metabolism-related protein (A and B) and gene (C), and relevant protein (D and E) and gene (F) expression in the liver of diabetic rats treated with alkylamides. Results are expressed as mean ± S.E.M (n=8). Conditions were as defined in Figure 2. Means with different superscript letters are significantly different among the diabetic rats (P< 0.05); $^{\#}$ means are significantly different (P<0.05) than the means in the control group. PEPCK: phosphoenolpyruvate

510 caboxykinase; G6Pase: glucose-6-phosphatase; GK: glucokinase; TRPV1: transient receptor
511 potential cation channel subfamily V member 1; CB1: cannabinoid receptor 1.
512 **Fig. 7** Insulin signaling-related protein (A and B) and gene (C), and relevant protein (D and E) and
513 gene (F) expression in the pancreas of diabetic rats treated with alkylamides. Results are expressed
514 as mean ± S.E.M (n=8). Conditions were as defined in Figure 2. Means with different superscript
515 letters are significantly different among the diabetic rats (P< 0.05); $^{\#}$ means are significantly
516 different (P<0.05) than the means in the control group. PDX-1: pancreatic duodenal homeobox-1;
517 GLUT2: glucose transporter 2; GK: glucokinase; TRPV1: transient receptor potential cation
518 channel subfamily V member 1; CB1: cannabinoid receptor 1.
519
520

521 **Fig.1**

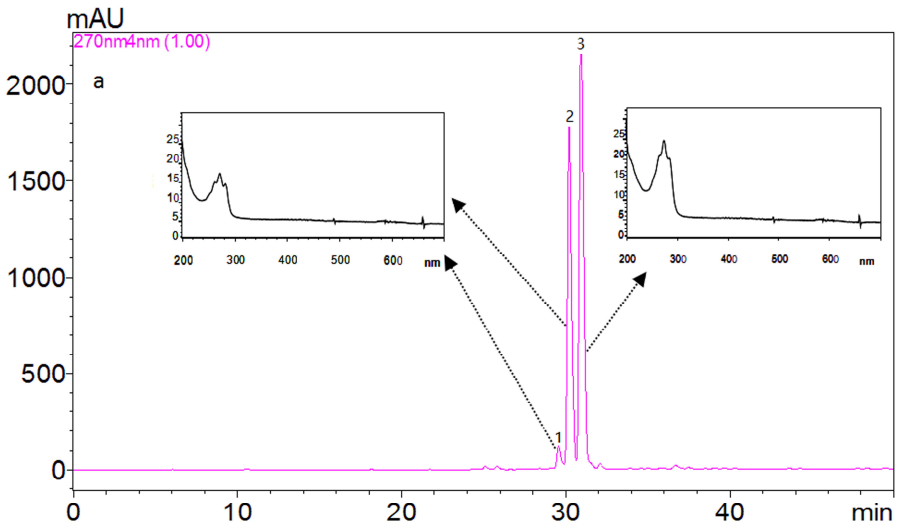

522

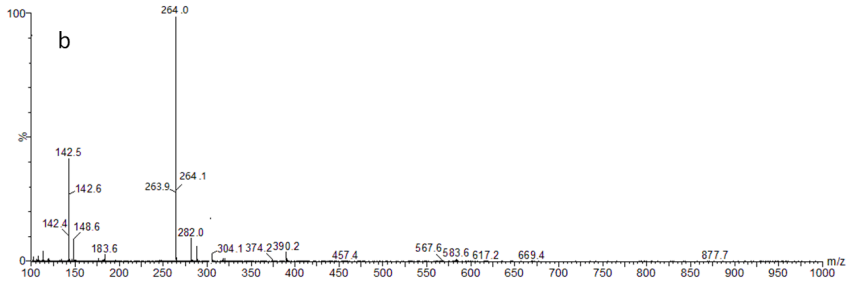

523

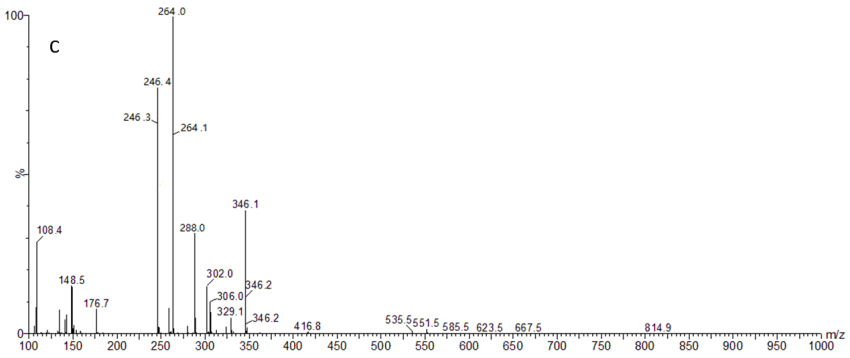

524

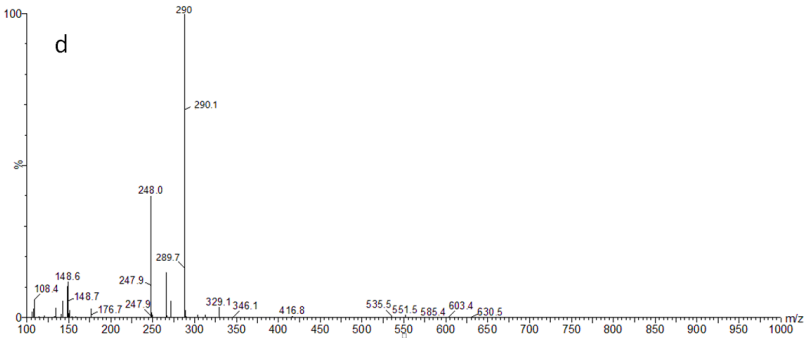

525

526

527 **Fig. 2**

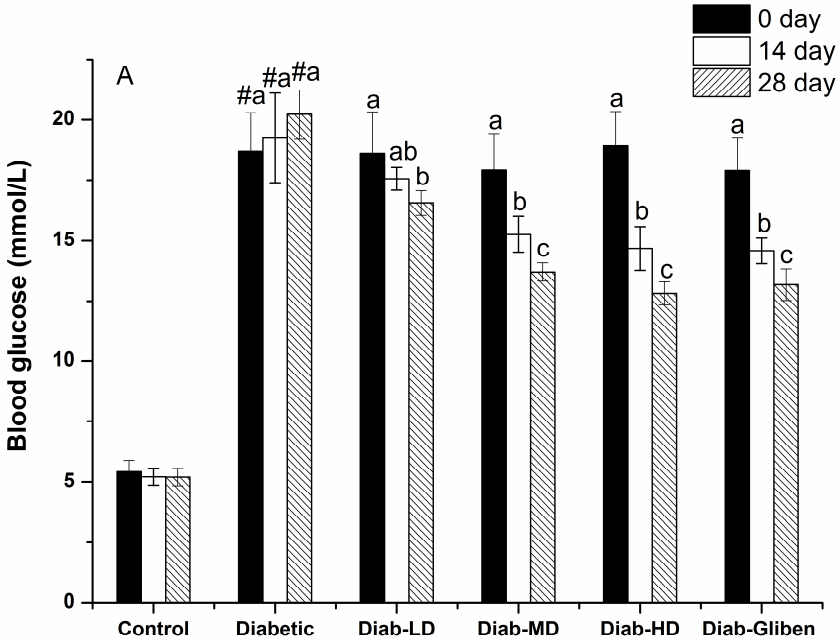

528

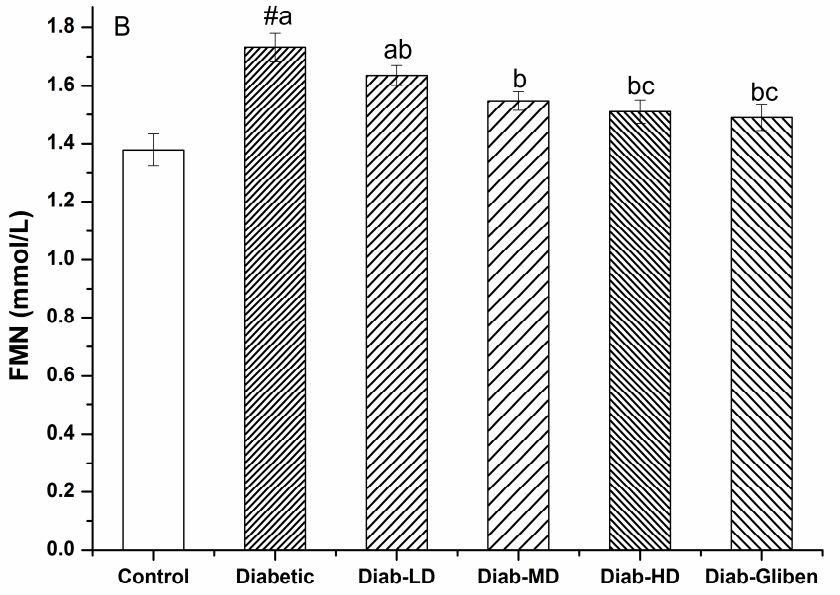

529

530

531 **Fig. 3**

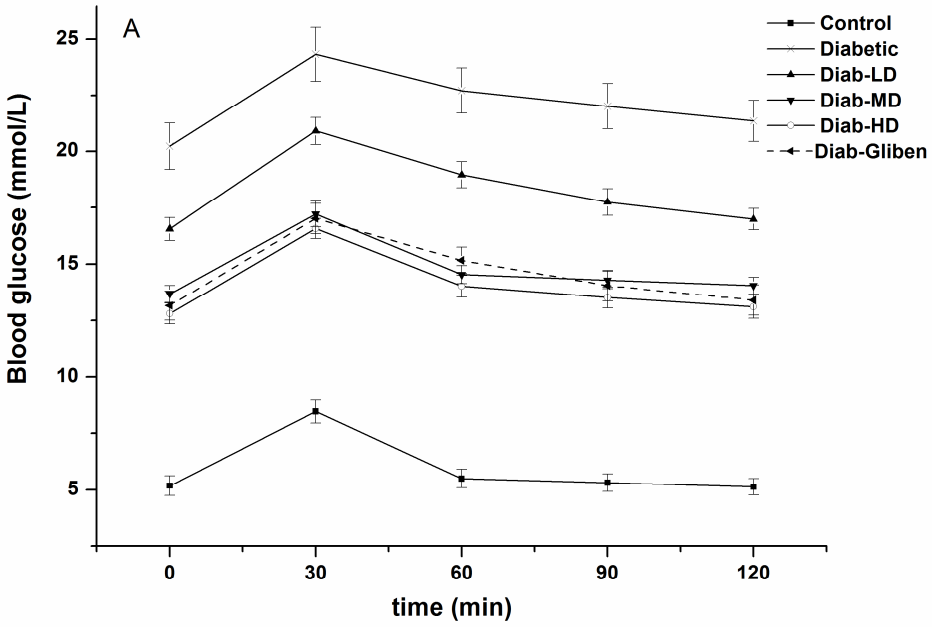

532

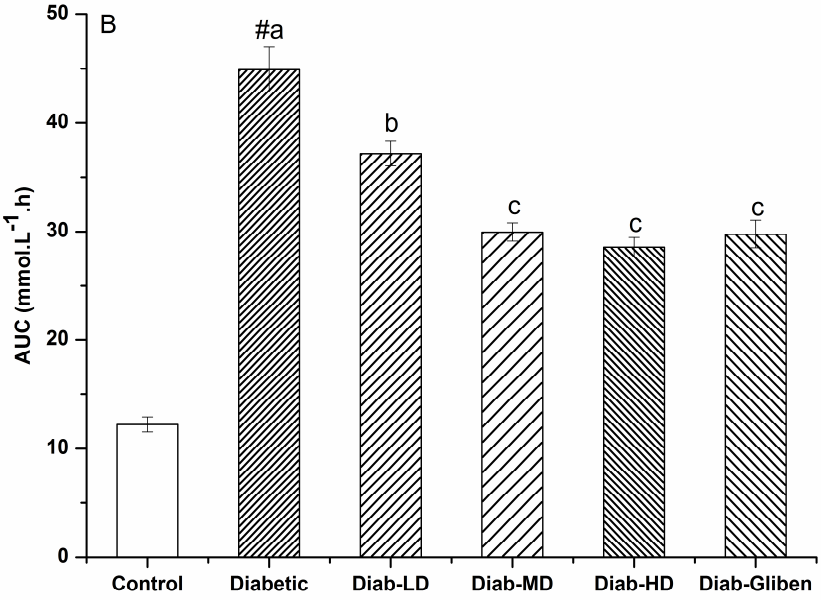

533

534

535 **Fig. 4**

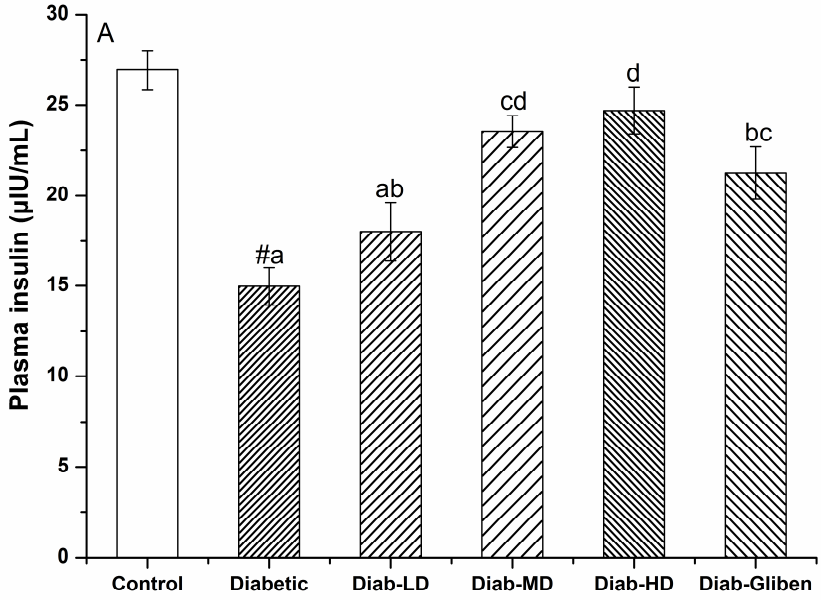

536

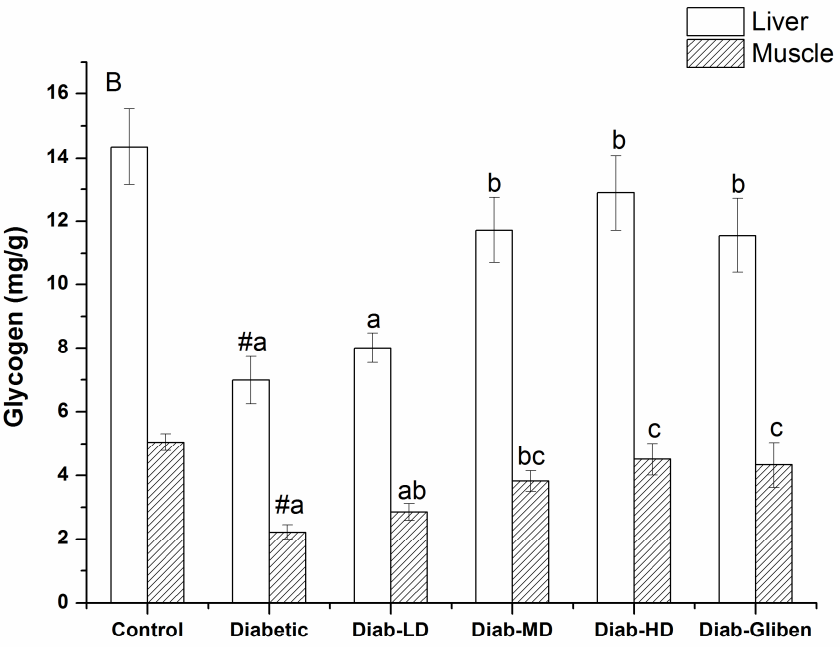

537

538

539 **Fig. 5**

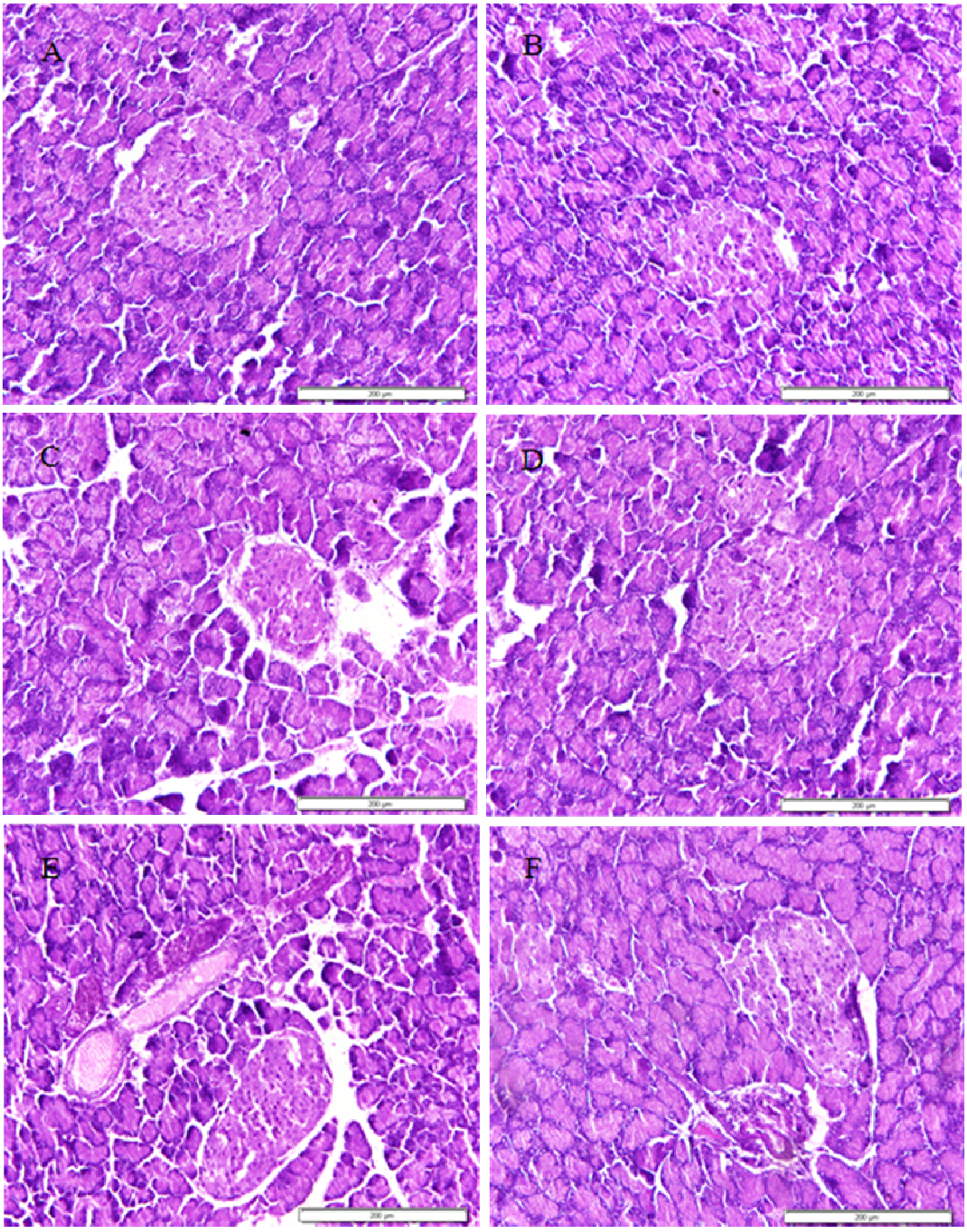

540
541

542 **Fig. 6**

543

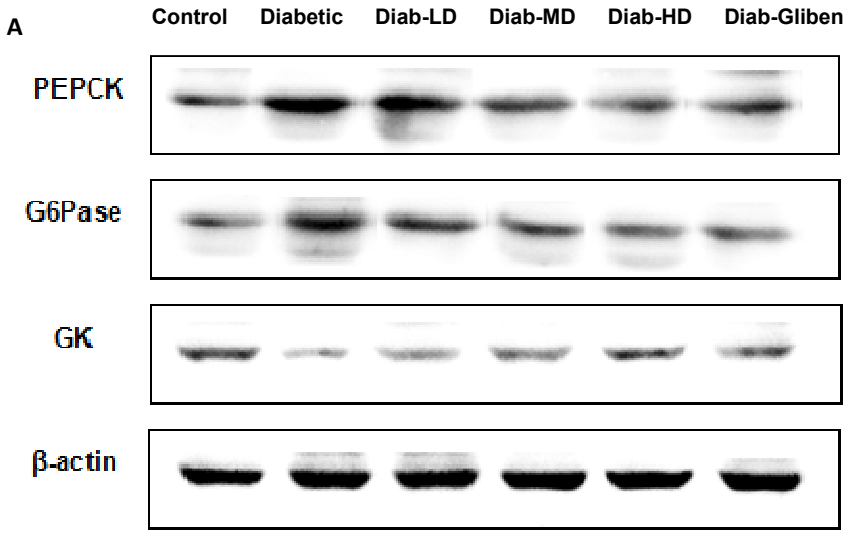

544

545

546

547

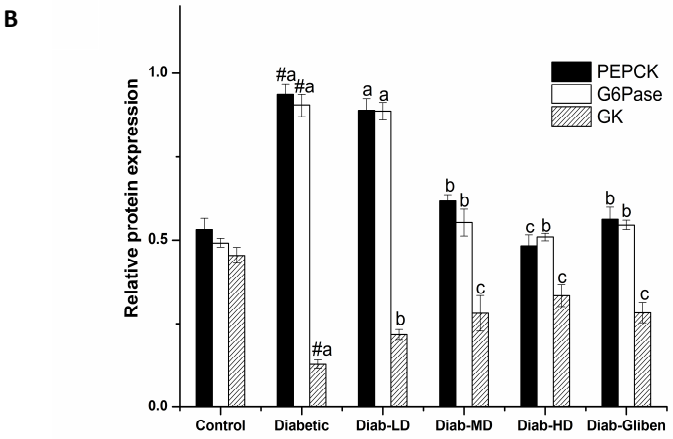

548

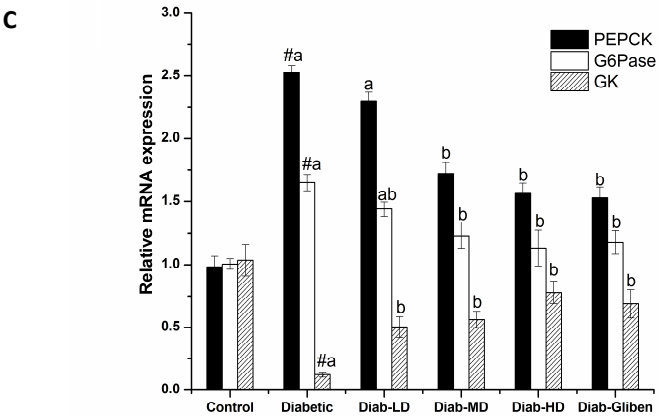

549

550

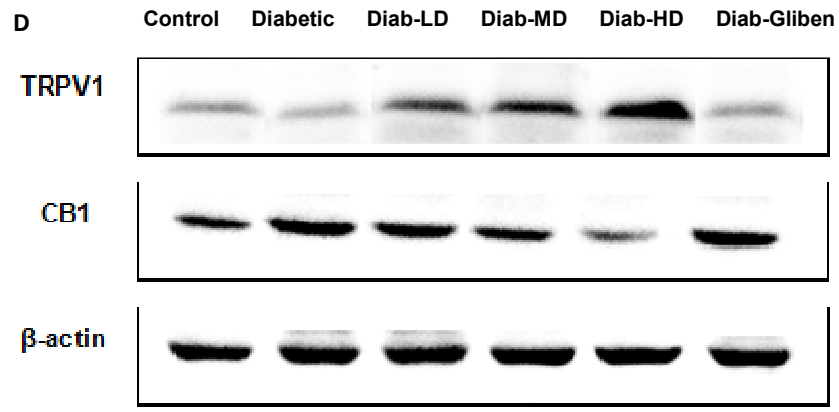

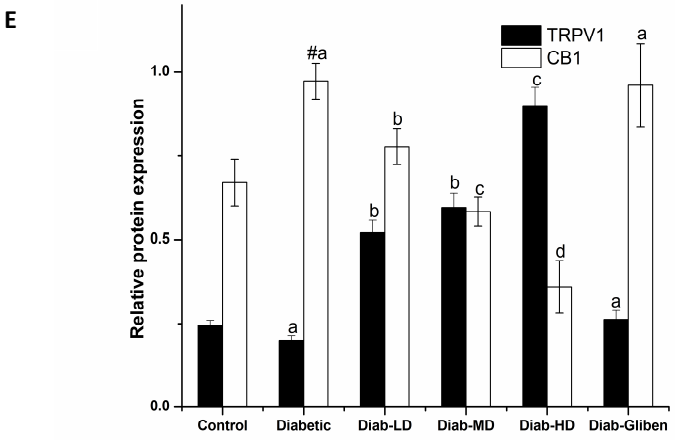

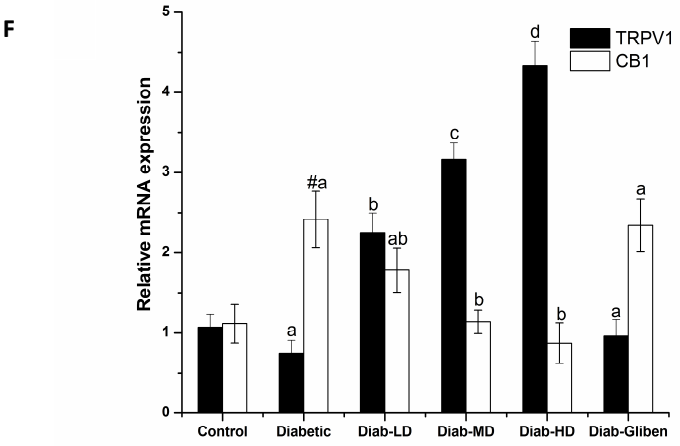

Fig. 7